Title

Improved ELISA for linoleate-derived diols in human plasma utilizing a polyHRP-based secondary tracer

Journal

Analytical Methods, 14(18)

ISSN

1759-9660

Authors

Singh, Nalin
Li, Dongyang
McReynolds, Cindy B
et al.

Publication Date

2022-05-13

DOI

10.1039/d2ay00272h

Peer reviewed

HHS Public Access

Author manuscript

Anal Methods. Author manuscript; available in PMC 2023 May 13.

Published in final edited form as:

Anal Methods. ; 14(18): 1810–1819. doi:10.1039/d2ay00272h.

Improved ELISA for linoleate-derived diols in human plasma utilizing a polyHRP-based secondary tracer

Nalin Singh[a], **Dongyang Li**[a], **Cindy B. McReynolds**[a], **Christophe Morisseau**[a], **Bruce D. Hammock**[*,a]

[a]Department of Entomology and Nematology and UC Davis Comprehensive Cancer Center, University of California Davis, Davis, California, 95616, USA

Abstract

Dihydroxyoctadecenoic acids (DiHOMEs) are cytochrome P450 pathway-derived metabolites of linoleic acid, a highly abundant dietary fatty acid. They serve thermogenic functions at low concentrations but, at high concentrations, are involved in proinflammatory and deleterious outcomes in a wide range of pathologies. Hence, the development of a reliable analytical method is critical to elucidate their potential as biomarkers of health, and enzyme-linked immunoassay (ELISA)-based approaches offer unique benefits as alternatives to traditional liquid chromatography-tandem mass spectrometry (LC-MS/MS) systems. Accordingly, an earlier ELISA for DiHOMEs was dramatically improved employing new secondary tracers and geared towards use in human plasma, a universal matrix in biomedical applications, as well as urine. Three ELISA formats, two utilizing polyHRP-based secondary labels for signal amplification, were compared. The best format involved a biotinylated detection antibody and a polyHRP-conjugated streptavidin tracer. Assay detectability was enhanced 20-fold, relative to the original immunoassay, and performance assessments validated precision, selectivity, and robustness. Fast and easy extraction-clean up steps yielded high analytical recovery and permitted the assay to operate in moderate concentrations (up to 20%) of plasma, expanding its practical relevance. Finally, the ELISA was applied towards detection of DiHOMEs in clinical samples and authenticated with complementary LC-MS/MS analysis. Hence, the method provides a valuable analytical tool to investigate the diverse and extensive roles of DiHOMEs in regulatory biology.

[*] bdhammock@ucdavis.edu; Tel: 530-752-7519.

Author contributions

Nalin Singh: conceptualization, methodology, validation, investigation, writing – original draft, writing – review & editing, visualization, funding acquisition. Dongyang Li: conceptualization, methodology, resources, supervision. Cindy B. McReynolds: resources, writing – review & editing, funding acquisition. Christophe Morisseau: methodology, resources, supervision. Bruce D. Hammock: conceptualization, resources, supervision, funding acquisition.

[†]Electronic Supplementary Information (ESI) available. See DOI: 10.1039/x0xx00000x

Ethics statement

All procedures for acquisition of plasma from human volunteers were in accordance with International Council for Harmonisation Good Clinical Practice guidelines and ethical principles that have their origin in the Declaration of Helsinki.

Conflicts of interest

B.D.H. and C.B.M. are employees of EicOsis LLC, a company that focuses on bringing soluble epoxide hydrolase inhibitors (such as EC5026) to the clinic for use as analgesics

Introduction

Linoleic acid (LA, 18:2) is the most abundant fatty acid in western diets and, consequently, one of the most prevalent in human adipose tissue.[1] It is an essential fatty acid,[2] required at low levels for endogenous synthesis of ω−6 polyunsaturated fatty acids (PUFAs), particularly arachidonic acid, and plays a critical role in maintenance of skin barrier function.[3] LA is a substrate of certain cytochromes P450 and is oxidized to epoxyoctadecenoic acids (EpOMEs).[4] EpOMEs consist of two regioisomers, the 9,10-EpOME and 12,13-EpOME, otherwise known as leukotoxin (LTX) and *iso*-leukotoxin (*iso*-LTX), respectively. They are hydrolyzed downstream by the soluble epoxide hydrolase (sEH) to the dihydroxyoctadecenoic acids (DiHOMEs), 9,10-DiHOME and 12,13-DiHOME, also known as leukotoxin diol (LTXD) and *iso*-leukotoxin diol (*iso*-LTXD), respectively.[4]

EpOMEs were initially termed LTXs due to their cytotoxicity and association with poor outcomes in burn and acute respiratory distress syndrome (ARDS) patients and model species.[5–7] However, studies utilizing EH-deficient systems and sEH inhibitors indicated hydrolytic bioactivation of LTXs is necessary for exertion of toxic effects, hence implicating the DiHOMEs (or LTXDs) as the deleterious agents.[8–10] DiHOMEs cause extensive vascular permeability[11] and are involved in inflammatory diseases,[12–15] pulmonary damage,[16] sepsis,[17] peroxisomal disorders,[18] and burn injury,[19] with high concentrations closely correlating with worsening morbidities. Recently, elevated plasma DiHOMEs were found to be excellent predictors of severe disease outcomes in patients with coronavirus disease 2019 (COVID-19).[20]

Conversely, at low concentrations, DiHOMEs in fact act as signaling mediators in areas of metabolic dysfunction and obesity, endocrine disruption, mitogenesis, pain perception, and immune response.[4] 12,13-DiHOME, in particular, modulates brown adipose tissue activation in response to cold exposure and exercise, enhances glucose and fatty acid uptake, and improves cardiac mitochondrial respiration.[21–23] Accordingly, it has been classified as a thermogenic batokine and lipokine as well. DiHOMEs were also present at excessively low levels in patients with certain heart disease.[23]

Hence, DiHOMEs appear to serve complex physiological roles, seemingly in a concentration-dependent manner. Thus, development of a validated analytical method with sufficient sensitivity to quantify a wide range of DiHOME concentrations is of considerable importance for their application as biomarkers of health and disease. Enzyme-linked immunosorbent assays (ELISA) are widely used for detection of a variety of analytes, including small molecules. While liquid chromatography-tandem mass spectrometry (LC-MS/MS) is the standard technique for multi-analyte analysis of oxidized lipids,[24,25] for single analytes, ELISAs offer distinct advantages such as a lower cost, ease of operation, simplicity, speed, and high-throughput implementations. They can also be adapted to a variety of sensor platforms for multiplex application, providing greater suitability for clinical investigations.

Previously, a competitive ELISA for DiHOMEs in urine was developed by our group.[26] In this study, the ELISA was modified and substantially improved utilizing new secondary labels (i.e., polymeric horseradish peroxidase (HRP)-based systems) for signal amplification and enhanced detectability. Furthermore, it was applied towards use in human plasma, a ubiquitous and clinically relevant matrix, in addition to urine. Three distinct ELISA formats were compared in parallel and method validation was conducted to ensure assay reliability. For the optimal format, selectivity, robustness, analytical recovery, and matrix effects in plasma were assessed. Finally, the method was applied towards clinical samples and verified with LC-MS/MS analysis.

Materials and methods

Reagents and instrumentation

Linoleic acid (LA) methyl ester, LA, and Ricinoleic acid (OLE) were purchased from NuChek Prep Inc. (Elysian, MN, USA). EpOMEs, 9,10-dihydroxystearic acid (9,10-DiHSA), 9,10-DiHOME, 12,13-DiHOME, dihydroxyoctadecdienoic acids (DiHODEs), dihydroxyeicosatrienoic acids (DiHETs), dihydroxydocosatrienoic acids (DiHDTs), dihydroxydocosapentaenoic acids (DiHDPs), and the tetrahydrofuran (THF)-diols of LA were prepared in-house.[24,27] Albumin from chicken egg white (Ovalbumin) was purchased from Millipore Sigma (St. Louis, MO, USA). All reagents for synthesis are commercially available and were purchased from one of the following vendors: Millipore Sigma, Fisher Scientific Company LLC (Pittsburg, PA, USA), or VWR International (Radnor, PA, USA). Methanol, 2-propanol, glacial acetic acid, hexanes, ethyl acetate (EtOAc), and acetonitrile of HPLC grade or better were purchased from Fisher Scientific. All chemicals purchased from commercial sources were used as received without further purification. Flash chromatography was performed on silica gel (230−400 Mesh, Grade 60) from Fisher Scientific. Analytical thin layer chromatography (TLC) was performed on TLC silica gel 60 F254 plates from Merck KGaA (Darmstadt, Germany). ^{1}H nuclear magnetic resonance (NMR) spectra were recorded on a 400 MHz Bruker Avance III HD Nanobay NMR spectrometer. High-resolution electrospray ionization mass spectrometry (HRESIMS) data were recorded on a Thermo Q-Exactive High-field Orbitrap mass spectrometer operating in negative ion mode. MS spectra of the coating antigen were recorded on the Orbitrap operating in positive ion mode. rProteinA GraviTrap Columns were purchased from Millipore Sigma. Zeba Spin Desalting/Buffer Exchange Columns were purchased from Fisher Scientific. EZ-Link Sulfo-NHS-LC-Biotin was purchased from Fisher Scientific. MaxiSorp clear flat-bottom immuno nonsterile 96-well plates were purchased from Fisher Scientific. Skim milk powder was purchased from Merck. HRP-conjugated Goat anti-Rabbit IgG was purchased from Jackson ImmunoResearch Laboratories Inc. (West Grove, PA, USA). Goat anti-Rabbit IgG PolyHRP40 and a Streptavidin PolyHRP40 Conjugate were purchased from Fitzgerald Industries International (Concord, MA, USA). 3,3′,5,5′-tetramethylbenzidine (TMB) was purchased from Millipore Sigma. The NanoDrop™ Lite Spectrophotometer for protein quantitation was purchased from Fisher Scientific. ELISA microplates were washed automatically with a 405 TS Microplate Washer from BioTek Instruments (Winooski, VT, USA). Microplate incubations were conducted with an MTS 2/4 digital microtiter shaker from IKA (Staufen, Germany). Optical density (O.D.) was

measured with a SpectraMax 190 Absorbance Microplate Reader from Molecular Devices (San Jose, CA, USA). UV-vis absorption spectra (200–800 nm) of the coating antigen were recorded with the SpectraMax Absorbance Reader. The Vortex-Genie 2 Mixer for solvent extraction/clean-up was purchased from Scientific Industries, Inc. (Bohemia, NY, USA). The accuSpin™ Micro 17R Microcentrifuge for solvent extraction/clean-up was purchased from Fisher Scientific.

Buffers and substrate

All buffers were prepared in Ultrapure water (18.1 MΩ/cm) from a MilliQ water purification system. For purification of the IgG antibody from antiserum, the binding, elution, and neutralization buffers were 20 mM sodium phosphate (pH 7.0), 0.1 M glycine-HCl (pH 3.0), and 1M Tris-HCl (pH 8.5), respectively. For the immunoassay, the coating buffer was 0.05 M sodium carbonate-bicarbonate (pH 9.6). The wash buffer was 1X phosphate-buffered saline (PBS, pH 7.4) containing 0.05% (v/v) Tween-20. The neat assay buffer was 1X PBS (pH 7.4). The TMB substrate solution for color development was prepared from three components, the substrate buffer (pH 3.8), a 1% H_2O_2 stock, and the TMB stock, as per a previously described method.[28]

Synthesis of DiHOME standard

The DiHOME standard (1:1 regioisomeric mixture, Fig. 1a) was synthesized as previously described.[24] Briefly, LA methyl ester was epoxidized with *meta*-chloroperoxybenzoic acid, followed by separation of the EpOME methyl esters by flash chromatography. The DiHOME methyl esters were obtained via perchloric acid-catalyzed hydrolysis of the epoxide. Finally, the free acid DiHOMEs were generated via base-catalyzed hydrolysis of the methyl ester and purified by flash chromatography. TLC plates (visualized with a $KMNO_4$ stain) revealed two conjoined spots, representing the two regioisomers ($R_f \approx 0.5$ in 60% Hexanes:40% EtOAc:0.2% glacial acetic acid developing solvent). ^{1}H NMR and HRESIMS data are described in the supplementary information. A stock solution of 1 mg/mL was prepared in acetonitrile, flushed with argon, and stored at −20 °C until use.

Purification of anti(α)-DiHOME antibody from rabbit antiserum

Antiserum active against DiHOMEs was from our group and was attained from an immunized rabbit as previously described.[26] The immunogen was a 9,10-/12,13-DiHOMEs-keyhole limpet hemocyanin (KLH) conjugate (Fig. 1b). Subsequently, the anti (α)-DiHOME IgG was purified from the antiserum via affinity chromatography with an rProteinA column, as per the manufacturer's instructions. Briefly, the column was first equilibrated with 10 mL binding buffer. 2 mL of antiserum was dissolved in 6 mL binding buffer and ran through the column (2x). After washing the column with 15 ml binding buffer, the IgG fraction was eluted with 4 ml elution buffer into tubes containing 20% (final v/v) neutralization buffer. Quantitation by spectrophotometry revealed isolation of 9.45 mg of total IgG. Following buffer exchange to PBS, the native antibody obtained (2.7 mg/mL) was aliquoted and stored at −20 °C until use.

Biotinylation of α-DiHOME antibody

Biotinylation of the α-DiHOME antibody was conducted utilizing sulfo-NHS-biotin-mediated coupling, as per the manufacturer's instructions. Briefly, fresh sulfo-NHS-biotin (10 equiv.) was added to the native antibody (1 equiv.) in PBS and the mixture was shaken for 1 h at room temperature. The solution was desalted (2x) to eliminate excess biotin and the biotinylated antibody (0.8 mg/mL) was aliquoted and stored at −20 °C until use.

Synthesis of coating antigen

The major structurally relevant coating antigens (cAg) had previously been screened by our group.[26] The optimal, heterologous cAg was identified as a ricinoleic acid (OLE)-ovalbumin (OVA) conjugate (Fig. 1c) and hence utilized for the current study. Briefly, the hapten (OLE, 1.0 equiv.) was activated with 1-Ethyl-3-(3-dimethylaminopropyl)carbodiimide (2.2 equiv.) and N-hydroxysuccinimide (1.4 equiv.) in anhydrous dimethylformamide by stirring under argon for 2 h at room temperature. The solution was then added dropwise to OVA in PBS and stirred overnight at room temperature for amine coupling. Protein desalting was conducted, and the cAg was aliquoted and stored at −20 °C until use. Characterization of OLE-OVA (MS, UV-vis spectra) is shown in Fig. S1.

Competitive enzyme-linked immunoassays

ELISA microplates were first coated with OLE-OVA (0.33–0.95 μg/mL, 100 μL/well in coating buffer) for 22 h at 4 °C. After plates were washed (300 μL/well wash buffer, 3x), wells were blocked (0.6 × g) with 3.5% (w/v) skim milk (250 μL/well in assay buffer) for 1 h at room temperature. Plates were washed again (300 μL/well, 3x) and the analyte (100 μL/well in assay buffer) was incubated with either the native (DetecAb) or biotinylated (BioAb) α-DiHOME antibody (100 ng/mL, 100 μL/well in assay buffer). The immunoreaction (0.6 × g) was allowed to proceed for 1 h at room temperature, after which plates were washed once again (300 μL/well, 3x). DetecAb was traced (0.6 × g) with either a monomeric HRP-linked or polymeric HRP (polyHRP)-linked goat α-rabbit IgG (100 ng/mL, 100 μL/well in assay buffer), while the BioAb was traced with the streptavidin-PolyHRP conjugate (100 ng/mL, 100 μL/well in assay buffer) for 30 min at room temperature. After a final set of washes (300 μL/well, 5x), the freshly prepared TMB substrate working solution (100 μL/well) was added and permitted to react (0.6 × g) for 15 min at room temperature (protected from light). The enzymatic action was quenched with 1 M H_2SO_4 (100 μL/well), plates were briefly shaken (10 sec), and absorbance was immediately read at λ_{Abs} = 450 nm.

Curve fitting

Calibration curves were constructed by plotting the O.D. values against the logarithm of the corresponding analyte concentration and fitted using OriginPro 8.5 software according to the 4-parameter logistic equation:

$$y = A2 + \frac{A1 - A2}{[1 + (x/x0)^{p}]}$$

A1 is the maximal O.D. at zero analyte concentration, A2 is the minimal O.D. at infinite analyte concentration, p is the slope at the inflection point, and x0 is the analyte concentration at which O.D. is 50% of the maximum (i.e., the IC_{50}). The linear working range is defined as the × values between which the O.D. is 20–80% of the maximum (i.e., the IC_{20}-IC_{80}), and was fitted according to the linear equation y = a + kx where k is the slope of the linear range. The limit of detection (LOD) was defined as the x value at which O.D. = $O.D._{\text{lowest standard point}} - [3 \times (\text{SD of } O.D._{\text{lowest standard point}})]$

Method validation

Intra- and inter-assay precisions were determined by the coefficients of variation (CV, SD/mean) for sample triplicates from one plate and means of samples from three plates (run on three separate days), respectively. The % background and signal-to-noise ratio (S/N) were calculated as (observed $O.D._{\cdot min}$/observed $O.D._{\cdot max}$) × 100 and upper asymptote (A1)/lower asymptote (A2), respectively.

Determination of cross-reactivity

Cross-reactivity (CR) was calculated as a relative IC_{50} value for the analyte compared to the DiHOME standard, as per the equation: % CR = (IC_{50} of DiHOME standard/IC_{50} of test analyte) × 100

Assessment of assay robustness

Calibration curves were prepared in a) assay buffer containing varying concentrations of methanol (5–50%, v/v), b) PBS buffer (pH 7.4) containing varying concentrations of Na_2HPO_4 (5–50 mM, 0.5X-5X), and c) 1X PBS buffer of varying pH values (pH 6.4–8.4). IC_{50} values and slopes of the linear range were compared to those of a calibration curve prepared in neat assay buffer (1X PBS, pH 7.4) to determine effects of an organic cosolvent, buffer ionic strength, and pH on ELISA performance, respectively.

Urine matrix tolerance

Calibration curves were prepared in assay buffer containing varying concentrations of spot human urine (5–50%, v/v) and compared to a calibration curve prepared in neat assay buffer to affirm serviceability of the ELISA in urine.

Extraction of DiHOMEs from plasma and extract clean-up

Human plasma (2 equiv.) was aliquoted into methanol (1 equiv.) and mixed strongly (10 sec) via a vortex mixer at maximal speed (34 × g). The solution was centrifuged at 4700 × g for 25 min. The precipitated pellet was discarded, and the collected supernatant was washed with hexanes (0.3 equiv., 3x). Briefly, the hexanes/aqueous-methanol mixture was vortexed strongly (10 sec, 34 × g) and centrifuged at 2200 × g for 5 min to partition the layers. The hexanes layer was carefully discarded, followed by addition of a fresh hexanes fraction for the next wash step. Finally, the cleaned extract was diluted in the assay buffer for the subsequent ELISA steps.

Spike recovery and matrix effects

For analytical recovery (AR) determinations, plasma samples were first pre-spiked with five concentrations of the standard (6.25, 12.5, 25, 50, and 100 ng/mL). Following MeOH extraction and clean-up, concentrations in extracts were calculated and compared to those of post-spike samples, as per the equation: % AR = ([DiHOMEs$_{\text{pre-spike}}$]/[DiHOMEs$_{\text{post-spike}}$]) × 100. For matrix effect (ME) assessments, post-extraction diluents with varying concentrations of plasma (2.5–50%, v/v in assay buffer) were spiked with the DiHOME standard. Slopes (k) of the linear range were determined and compared to the k of a diluent prepared in neat assay buffer, as per the equation: % ME = ({k$_{\text{post-spike plasma}}$ − k$_{\text{neat blank}}$}/k$_{\text{neat blank}}$) × 100. Negative or positive deviations were indicative of signal suppression or enhancement, respectively.

Real-sample analysis

In order to determine the ability of the assay to detect DiHOME concentrations in clinical samples, plasma obtained from healthy human volunteers who had undergone a clinical trial was analyzed using the developed ELISA. This clinical study (NCT04908995) had been conducted in accordance with International Council for Harmonisation Good Clinical Practice guidelines and ethical principles that have their origin in the Declaration of Helsinki. Briefly, volunteers had been dosed with either a placebo or EC5026 (an sEH inhibitor), followed by *ex vivo* treatment of collected whole blood samples with lipopolysaccharides (LPS). An aliquot of the plasma fraction of whole blood isolated post-treatment was acquired and utilized for detection of DiHOMEs by the method described above.

Confirmation by LC-MS/MS

LC-MS/MS analysis of real samples was conducted on an Agilent 1200 Series high-performance LC (HPLC) system from Agilent Technologies Inc. (Santa Clara, CA, USA), coupled to a SCIEX 4000 Q-TRAP tandem mass spectrometer from Applied Biosystems (Waltham, MA, USA), equipped with an electrospray ionization source (Turbo V), and operating in negative multiple reaction monitoring (MRM) mode. 10 μL of samples were injected onto a reverse-phase 2.1 mm × 100 mm, 1.7 μm Kinetex C18 column, held at 40 °C. A gradient elution (Table S1), with a constant flow rate of 250 μL/min, was employed for a 7 min chromatographic run (t_R of 3.08 and 3.13 min for 12,13- and 9,10-DiHOME, respectively). Mobile phase A was water with 0.1% glacial acetic acid and mobile phase B was methanol:2-propanol (1:1) with 0.1% glacial acetic acid. The distinctive MRM transitions monitored were *m/z* 313 (Q1) to *m/z* 183 ($Q3_a$) and *m/z* 201 ($Q3_b$) for 12,13- and 9,10-DiHOME, respectively, as previously identified.[29] Q-TRAP conditions and tandem MS parameters are described in Tables S2–S3.

Results and discussion

Comparison of three ELISA formats

Three competitive ELISA formats, A-C (Fig. 2), each utilizing a unique secondary label and performed in parallel with equivalent reagent concentrations, were investigated. Ideal

concentrations of coating antigen and primary antibody were identified by a checkerboard titration (Fig. S2) and were determined to be 0.95 μg/mL (ppm) and 0.1 μg/mL, respectively. Moreover, the optimal concentration of secondary tracers was 0.1 μg/mL. In formats A and B, the native α-DiHOME antibody (DetecAb) was used to bind the antigen. Taking advantage of the minimal influence of biotinylation on antibody function,[30] a biotinylated variant (BioAb) was utilized in format C. The DetecAb in format A was traced with a monomeric HRP-linked α-rabbit IgG. In contrast, formats B and C employed polyHRP-coupled secondary tracers for desired signal amplification, which would be expected due to the augmented specific activity of enzyme conjugates that results from the higher number of enzyme molecules present.[30,31] A polyHRP-linked α-rabbit IgG was used in format B, while a streptavidin (SA)-polyHRP complex was utilized in format C, capitalizing on the exceptionally strong biochemical affinity between SA and biotin.[30,31]

The acquired IC_{50} values for all three formats were in the range of 0.57–0.77 ng/mL (Fig. 3), compared to the IC_{50} of 8 ng/mL for the original DiHOME ELISA.[26] This signifies a 10–15-fold increase in assay detectability, driven largely by application of new and enhanced secondary tracers. Importantly, for the polyHRP-based layouts B and C, the sizable improvement in detectability was attained without sacrificing signal magnitude (Fig. 3) as the maximum O.D. values observed (0.84–1.50) were comparable to that of the initial assay (0.86).[26]

At equal reagent concentrations, there were few differences in the LOD, IC_{50}, and scope of the linear ranges (IC_{20}-IC_{80}) between format A and formats B and C (Table 1). Nevertheless, as noted, the signal response was considerably larger for the latter two formats (maximum O.D. of 0.84–1.50 vs. 0.39 for format A), a result of stronger polyHRP-mediated signal generation. Most prominently, the slopes of the linear range (k) for formats B and C were 2-fold and 4.5-fold greater than the k of format A, respectively (Table 1). Since k is defined as $dO.D./d[Analyte]$ and is hence a measure of assay sensitivity,[30] the steeper slopes indicate substantially greater discriminating power for the polyHRP systems, especially format C. In contrast, parameters such as background and S/N were only marginally better for the polyHRP setups (Table 2). All three layouts possessed high intra- and inter-assay precision, validating their reliability, with the lowest CV seen for format C (Table 2). Altogether, primarily based on its highest amplification factor (i.e., ratio of k) and thus relative sensitivity,[30] the BioAb-SA-polyHRP configuration (i.e., format C) was considered optimal and adopted for further experiments.

Optimization of detectability

Because of the signal magnification afforded by the polyHRP label in ELISA format C, coating antigen (cAg) concentrations were lowered to further enhance assay detectability. Lessening the cAg typically decreases the IC_{50} of competitive immunoassays,[32] due to the increase in specificity of antibody binding. Fittingly, decreasing [cAg] by 30–50% drove down IC_{50} values sizably (0.47–0.39 ng/mL vs. 0.70 ng/mL, Fig. 4), while retaining suitable signal strength ($O.D._{max}$ = 1.23–0.94). However, an excessive reduction (70%) in [cAg] resulted in undesirable loss of signal ($O.D._{max}$ = 0.69) without any appreciable improvement in IC_{50} (0.37 ng/mL). Hence, relatively moderate concentrations of cAg were

considered optimal and yielded an ELISA with a 20-fold greater detectability than the original method.[26]

Selectivity

A cross-reactivity assessment with structurally related and biologically relevant fatty acids was conducted to ensure selectivity of the ELISA towards the target DiHOMEs (Table 3). Most critically, the ELISA did not cross-react with either linoleic acid (LA) or EpOMES (< 0.1%), indicating that the upstream precursors of DiHOMEs would not impede their detection. There was also insignificant cross-reactivity towards the THF-diols of LA (1.19%), alternative oxidized metabolites of EpOMEs.[27,33] Expectedly, the assay exhibited a degree of cross-reactivity for OLE, a component of the coating antigen (Fig. 1c), though it was small (11.9%). Cross-reaction with other dihydroxy fatty acids (DiHFAs) from common fatty acids was also assessed. It was negligible towards 9,10-DiHSA (0.54%), the diol derived from the abundant monounsaturated fatty acid, oleic acid (18:1). Cross-reactivity was low for ω-3-based DiHFAs, namely Docosahexaenoic acid (22:6)-derived DiHDPs (6.10%) and ω-3 alpha-linolenic acid (18:3)-derived DiHODEs (14.3%), although the relatively higher recognition for the latter is potentially due to greater structural homology. Highest cross-reactivity was seen towards ω−6 arachidonic acid (20:4)-derived DiHETs (30.0%) and their dihomo- analogues, adrenic acid (22:4)-derived DiHDTs (38.7%). This is perhaps because of the intersecting ω-6 nature of these diols, recalling that LA is the precursor for synthesis of the parent fatty acids. Still, since endogenous concentrations of linoleate metabolites far exceed those of corresponding metabolites derived from arachidonate,[34] the impact of this moderate non-selectivity would be trivial in real sample analyses.

Organic cosolvent, ionic strength, and pH tolerance

Since methanol (MeOH) was employed as the organic cosolvent for extraction of DiHOMEs from plasma (as discussed in a later section), its impact on ELISA performance was evaluated. Low-moderate concentrations of MeOH (5–20%) had a limited effect on calibration curves and k values (Fig. 5a), relative to the neat assay buffer, though IC_{50} values did increase slightly at moderate MeOH concentrations (10–20%). A high concentration (50%), however, distorted the calibration curve (10-fold jump in IC_{50}) and flattened out the k, implying major interference. Hence, ELISA performance was retained and considered functional in assay buffer containing a concentration of up to 20% MeOH. Another consideration is the ionic strength of the PBS buffer. Relative to the standard concentration of phosphate buffer (10 mM Na_2HPO_4, 1X), lower (5 mM, 0.5X) or moderately higher (20 mM, 2X) concentrations did not significantly hamper the ELISA (Fig. 5b), though k and $O.D._{max}$ did begin to drop at the latter concentration. A considerably more concentrated buffer (50 mM, 5X) adversely impacted the ELISA with a 2-fold reduction in k and diminished signal magnitude, suggesting that assay performance declines with increasing buffer ionic strength. Effects of pH fluctuations, ranging from slight acidity (pH 6.4) to slight basicity (pH 8.4), were also examined. The ELISA tolerated pH shifts in both directions quite well with minimal alterations to k and IC_{50} values (Fig. 5c), relative to neutral conditions (pH 7.4), suggesting resiliency against mildly acidic and alkaline conditions.

Solvent extraction, analytical recovery, and plasma tolerance

The original DiHOMEs ELISA was developed for application in urine samples since DiHOMEs can be metabolized and excreted as glucuronides and other conjugates.[26] Accordingly, functionality of the current assay was verified in human urine (useable in up to concentrations of 10%) and matching augmentations in detectability (i.e., greater than one order of magnitude reductions in the IC_{50}) were achieved (Fig. S3), indicating that the improved ELISA is also suitable for analysis of DiHOMEs in this pertinent matrix.

Nevertheless, the emphasis of the present method was on human plasma as the matrix since it is of greatest clinical relevance. Assessment and mitigation of matrix effects are key considerations to verify relevance of an assay towards real sample analysis. Typically, dilution into the assay buffer is the primary and simplest mode to reduce matrix influences. However, plasma is a complex medium with multiple polar and nonpolar elements that can adversely impact assay functionality. Hence, a quick and straightforward two-step extraction-clean-up process was employed first, to enhance sample quality and decrease the degree of dilution required for reliable method performance. In the extraction step, plasma was aliquoted into methanol, a water-miscible organic solvent commonly used as a cosolvent in ELISAs due to its relatively low influence on antigen-antibody interactions.[35] This extraction minimizes interference from salts and proteins (by precipitating them out) and apportions the DiHOMEs into the supernatant fraction. In the clean-up step, the methanol-aqueous extract was washed with hexanes, an immiscible nonpolar solvent. This was conducted to remove the potentially intrusive lipophilic components of plasma, while permitting retention of DiHOMEs in the polar layer, in accordance with the preferential partitioning of DiHFAs.[36]

An analytical recovery of around 100% at five concentration levels of DiHOMEs validated this approach (Table 4), indicating efficient extraction and reliable retrieval of DiHOMEs from human plasma. Furthermore, investigations of matrix effects revealed that low-moderate plasma concentrations (2.5–20%) did not significantly impact assay performance (Table 5). This is of particular significance since it suggests that the ELISA is operational in plasma samples after only a 5-fold-dilution, increasing potential for analysis of biological systems where DiHOMEs are present at lower concentrations. This contrasts with assays which possess high detectability in assay buffer but require 20–100-fold dilutions to be functional in real samples, a factor that restricts their tangible detection limits. However, a high plasma concentration (50%) did still result in substantial signal suppression (≈ 60%) for the method (Table 5).

Detection of DiHOMEs in real samples and correlation with LC-MS/MS analysis

Lastly, DiHOMEs were detected in plasma obtained from participants of a clinical trial for an sEH inhibitor (i.e., EC5026), to verify applicability of the developed ELISA towards clinical samples. DiHOMEs were successfully quantified in four different treatment groups (Fig. 6a), verifying pertinence of the ELISA towards real-sample analyses. Samples were also analyzed by LC-MS/MS to independently verify the detection of DiHOMEs with the previously validated analytical technique. Findings demonstrated a strong correlation

(Pearson's coefficient of correlation, r = 0.961, Fig. 6b) between concentrations across the two methods, further bolstering reliability of the ELISA method.

Conclusions

Herein, an enhanced competitive ELISA for detection of linoleic acid-derived diols was developed. Employment of a new secondary tracer improved detectability by more than one order of magnitude and various performance evaluations verified assay reliability. Tolerance to moderate concentrations of the plasma matrix and good correlation with LC-MS/MS with respect to analysis of clinical samples verified translatability for practical applications.

Differentiating the detectability between DiHOME regioisomers revealed that, intriguingly, the assay displays far greater selectivity for 12,13-DiHOME (≈ 23-fold, Fig. 7), even though the original immunizing agent was a 9,10-/12,13-DiHOME (1:1)-KLH conjugate (Fig. 1b), suggesting strong regioisomeric-preference. This observation is likely due in part to the coating antigen used (Fig. 1c). Reactivity towards 9,10-DiHOME is sufficient enough for it to be detectable in samples with high levels of DiHOMEs but recognition would fall below the detection limit in samples with low to moderate concentrations. On the contrary, as illustrated, the ELISA exhibits excellent sensitivity towards 12,13-DiHOME, which tends to be the endogenously predominant regioisomer[34] and has been associated with a broader range of biologies.[14,15,19,21–23] Incidentally, there is a commercially available competitive ELISA kit for 12,13-DiHOME (Cayman Chemical #501720). Nonetheless, the current assay possesses considerably greater detectability (≈ 7-fold higher than reported value) towards 12,13-DiHOME and is significantly more economical.

Therefore, as a next step, development of a 9,10-DiHOME-specific assay, potentially utilizing a different immunogen and/or coating antigen, could be explored for separate detection of this regioisomer since it might have some distinct biological activities. Moreover, there is growing interest in monoclonal single chain antibodies (or nanobodies) for detection of small molecules by immunoassay due to their higher specificity, relative to conventional IgG antibodies.[31,37] Hence, nanobody-based ELISAs could be considered for regioisomer differentiation and comparable (or even enhanced) assay detectability.

While the method established in this study is far superior to older and commercially available immunoassays for DiHOMEs, its analytical performance would be unable to match that of traditionally used LC-MS/MS instruments. The LC-MS/MS methods previously reported boast an even greater sensitivity[38] (LOD of 0.0004–0.002 ng/mL vs. 0.05 ng/mL for ELISA) and a much larger linear working range[39] (four orders-of-magnitude difference between upper and lower limits vs. one order for ELISA), as well as permit synchronous differentiation of both regioisomers[29] (based on different fragmentation patterns, retention times). Thus, LC-MS/MS technology remains the gold standard for bioanalysis of DiHOMEs (and other oxidized lipids). However, its expensive and cumbersome nature can limit its applicability and hence the developed ELISA offers a fast and cheap alternative for high-throughput analyses, making it particularly suited for a clinical setting. Finally, the ELISA could be incorporated into multiplex platforms for simultaneous detection with other

biomarkers of health and disease for a holistic evaluation of biological mechanisms and phenotypic outcomes.

Supplementary Material

Refer to Web version on PubMed Central for supplementary material.

Acknowledgments

This work was partially supported by National Institutes of Health grants, National Institute of Environmental Health Sciences (NIEHS) RIVER Award R35 ES030443-01 (to B.D.H.), NIEHS Superfund Award P42 ES004699 (to B.D.H.), National Institute of General Medical Sciences (NIGMS) T32GM113770 (to C.B.M.), and National Heart, Lung, and Blood Institute (NHLBI) T32HL086350 (to N.S.).

References

1. Guyenet SJ and Carlson SE, Adv Nutr, 2015, 6, 660–664. [PubMed: 26567191]
2. Lands B, Prog. Lipid Res, 2022, 85, 101142. [PubMed: 34818526]
3. Chiba T, Thomas CP, Calcutt MW, Boeglin WE, O'Donnell VB and Brash AR, J. Biol. Chem, 2016, 291, 14540–14554. [PubMed: 27151221]
4. Hildreth K, Kodani SD, Hammock BD and Zhao L, J. Nutr. Biochem, 2020, 86, 108484. [PubMed: 32827665]
5. Suzuki K, Aoyama H, Izawa Y, Kobayashi M and Ozawa T, Burns, 1981, 8, 110–117.
6. Kosaka K, Suzuki K, Hayakawa M, Sugiyama S and Ozawa T, Mol. Cell. Biochem, 1994, 139, 141–148. [PubMed: 7862104]
7. Ozawa T, Sugiyama S, Hayakawa M, Satake T, Taki F, Iwata M and Taki K, Am. Rev. of Respir. Dis, 1988, 137, 535–540. [PubMed: 3345035]
8. Moghaddam MF, Grant DF, Cheek JM, Greene JF, Williamson KC and Hammock BD, Nat. Med, 1997, 3, 562–566. [PubMed: 9142128]
9. Greene JF, Newman JW, Williamson KC and Hammock BD, Chem. Res. Toxicol, 2000, 13, 217–226. [PubMed: 10775319]
10. Zheng J, Plopper CG, Lakritz J, Storms DH and Hammock BD, Am. J. Respir. Cell Mol, 2001, 25, 434–438.
11. Slim R, Hammock BD, Toborek M, Robertson LW, Newman JW, Morisseau CHP, Watkins BA, Saraswathi V and Hennig B, Toxicol. Appl. Pharmacol, 2001, 171, 184–193. [PubMed: 11243918]
12. Samokhvalov V, Jamieson KL, Darwesh AM, Keshavarz-Bahaghighat H, Lee TYT, Edin M, Lih F, Zeldin DC and Seubert JM, Front. Pharmacol, 2019, 9, 1572. [PubMed: 30692927]
13. Smith KR, Pinkerton KE, Watanabe T, Pedersen TL, Ma SJ and Hammock BD, Proc. Natl. Acad. Sci. U.S.A, 2005, 102, 2186. [PubMed: 15684051]
14. Zimmer B, Angioni C, Osthues T, Toewe A, Thomas D, Pierre SC, Geisslinger G, Scholich K and Sisignano M, Biochim. Biophys. Acta - Mol. Cell Biol. Lipids, 2018, 1863, 669–678. [PubMed: 29625231]
15. Levan SR, Stamnes KA, Lin DL, Panzer AR, Fukui E, McCauley K, Fujimura KE, McKean M, Ownby DR, Zoratti EM, Boushey HA, Cabana MD, Johnson CC and Lynch SV, Nat. Microbiol, 2019, 4, 1851–1861. [PubMed: 31332384]
16. Ishizaki T, Ozawa T and Voelkel NF, Pulm Pharmacol Ther, 1999, 12, 145–155. [PubMed: 10419834]
17. Hamaguchi M, Wu HN, Tanaka M, Tsuda N, Tantengco OAG, Matsushima T, Nakao T, Ishibe T, Sakata I and Yanagihara I, Acute Medicine & Surgery, 2019, 6, 413–418.
18. Street JM, Evans JE and Natowicz MR, J. Biol. Chem, 1996, 271, 3507–3516. [PubMed: 8631955]
19. Bergmann CB, McReynolds CB, Wan D, Singh N, Goetzman H, Caldwell CC, Supp DM and Hammock BD, Proc. Natl. Acad. Sci. U.S.A, 2022, 119, e2120691119. [PubMed: 35312372]

20. McReynolds CB, Cortes-Puch I, Ravindran R, Khan IH, Hammock BG, Shih P.-a. B., Hammock BD and Yang J, Front. Physiol, 2021, 12, 403.
21. Lynes MD, Leiria LO, Lundh M, Bartelt A, Shamsi F, Huang TL, Takahashi H, Hirshman MF, Schlein C, Lee A, Baer LA, May FJ, Gao F, Narain NR, Chen EY, Kiebish MA, Cypess AM, Blüher M, Goodyear LJ, Hotamisligil GS, Stanford KI and Tseng Y-H, Nat. Med, 2017, 23, 1384–1384.
22. Stanford KI, Lynes MD, Takahashi H, Baer LA, Arts PJ, May FJ, Lehnig AC, Middelbeek RJW, Richard JJ, So K, Chen EY, Gao F, Narain NR, Distefano G, Shettigar VK, Hirshman MF, Ziolo MT, Kiebish MA, Tseng Y-H, Coen PM and Goodyear LJ, Cell Metab, 2018, 27, 1111–1120.e1113. [PubMed: 29719226]
23. Pinckard KM, Shettigar VK, Wright KR, Abay E, Baer LA, Vidal P, Dewal RS, Das D, Duarte-Sanmiguel S, Hernández-Saavedra D, Arts PJ, Lehnig AC, Bussberg V, Narain NR, Kiebish MA, Yi F, Sparks LM, Goodpaster BH, Smith SR, Pratley RE, Lewandowski ED, Raman SV, Wold LE, Gallego-Perez D, Coen PM, Ziolo MT and Stanford KI, Circulation, 2021, 143, 145–159. [PubMed: 33106031]
24. Newman JW, Watanabe T and Hammock BD, J. Lipid Res, 2002, 43, 1563–1578. [PubMed: 12235189]
25. Yuan Z-X, Majchrzak-Hong S, Keyes GS, Iadarola MJ, Mannes AJ and Ramsden CE, Anal. Bioanal. Chem, 2018, 410, 6009–6029. [PubMed: 30074088]
26. Zurek G, Gee SJ and Hammock BD, Anal. Chim. Acta, 2002, 466, 247–256.
27. Moghaddam MF, Motoba K, Borhan B, Pinot F and Hammock BD, Biochim. Biophys. Acta – Gen. Subj, 1996, 1290, 327–339.
28. Li D, Morisseau C, McReynolds CB, Duflot T, Bellien J, Nagra RM, Taha AY and Hammock BD, Anal. Chem, 2020, 92, 7334–7342. [PubMed: 32253910]
29. Bylund J, Ericsson J and Oliw EH, Anal. Biochem, 1998, 265, 55–68. [PubMed: 9866708]
30. Li D, Ying Y, Wu J, Niessner R and Knopp D, Microchim Acta, 2013, 180, 711–717.
31. Li D, Cui Y, Morisseau C, Gee SJ, Bever CS, Liu X, Wu J, Hammock BD and Ying Y, Anal. Chem, 2017, 89, 6248–6256. [PubMed: 28460522]
32. Wang X, Cohen L, Wang J and Walt DR, J. Am. Chem. Soc, 2018, 140, 18132–18139. [PubMed: 30495929]
33. Markaverich Barry M, Alejandro M, Thompson T, Mani S, Reyna A, Portillo W, Sharp J, Turk J and Crowley Jan R, Environ. Health Perspect, 2007, 115, 702–708. [PubMed: 17520056]
34. Schmöcker C, Zhang IW, Kiesler S, Kassner U, Ostermann AI, Steinhagen-Thiessen E, Schebb NH and Weylandt K-H, Int. J. Mol. Sci, 2018, 19, 180.
35. Cui X, He Q, Shen D, Jiang Z, Chen Y, Zhao S and Hammock BD, Anal. Methods, 2018, 10, 2629–2635.
36. Gill SS, Ota K and Hammock BD, Anal. Biochem, 1983, 131, 273–282. [PubMed: 6614459]
37. Li Z-F, Dong J-X, Vasylieva N, Cui Y-L, Wan D-B, Hua X-D, Huo J-Q, Yang D-C, Gee SJ and Hammock BD, Sci. Total Environ, 2021, 753, 141950. [PubMed: 32906044]
38. Mastrogiovanni M, Trostchansky A, Naya H, Dominguez R, Marco C, Povedano M, López-Vales R and Rubbo H, Biomedicines, 2022, 10, 674. [PubMed: 35327476]
39. Gouveia-Figueira S, Späth J, Zivkovic AM and Nording ML, PLoS One, 2015, 10, e0132042–e0132042. [PubMed: 26186333]

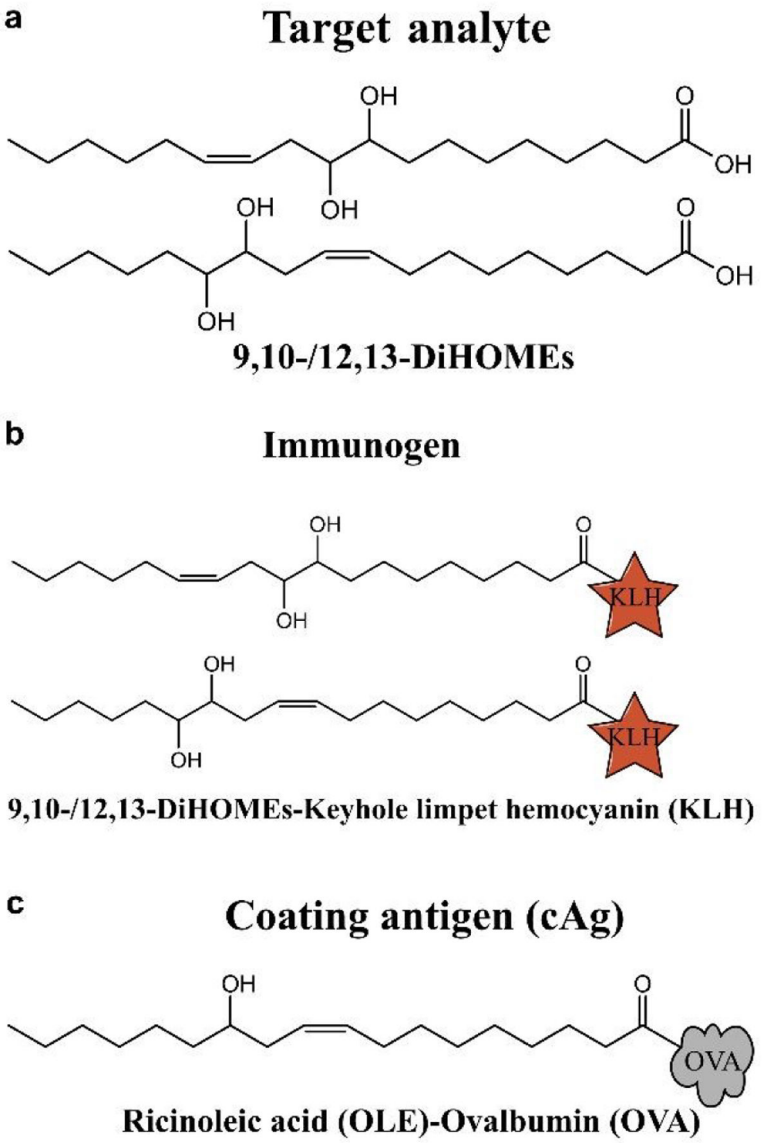

Fig. 1.

Structures of the (a) target analyte standard, (b) immunogen,[26] and (c) coating antigen employed for development of the DiHOMEs ELISA

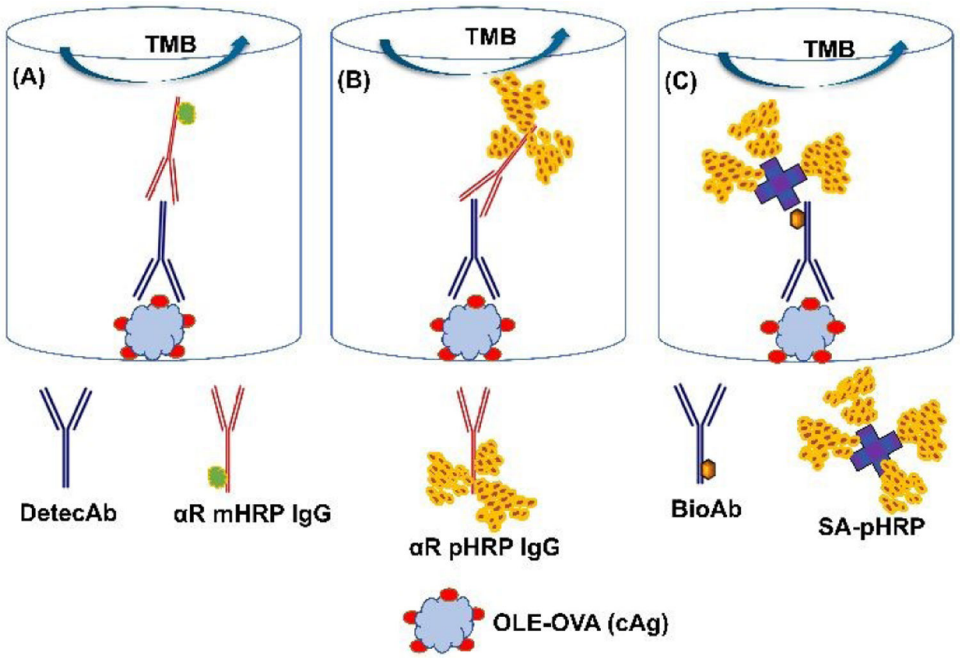

Fig. 2.

Schematic of three competitive ELISA formats for DiHOMEs. (A) The native anti(α)-DiHOME antibody (DetecAb) was traced with a monomeric HRP-linked α-rabbit IgG (αR mHRP IgG). (B) The DetecAb was traced with a polymeric HRP-linked α-rabbit IgG (αR pHRP IgG). (C) The biotinylated α-DiHOME antibody (BioAb) was traced with a streptavidin-polyHRP complex (SA-pHRP). Illustrations are representative of the substrate-mediated color development step (post-washes).

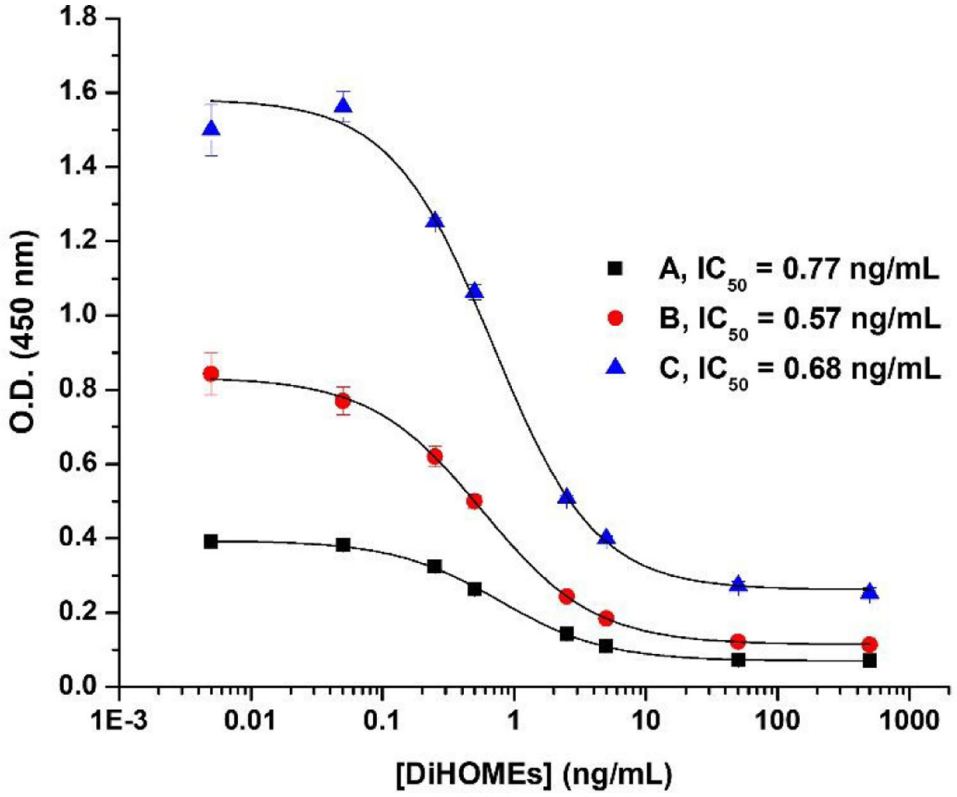

Fig. 3.
Calibration curves (and IC_{50} values) of the three ELISA formats A-C in neat assay buffer.

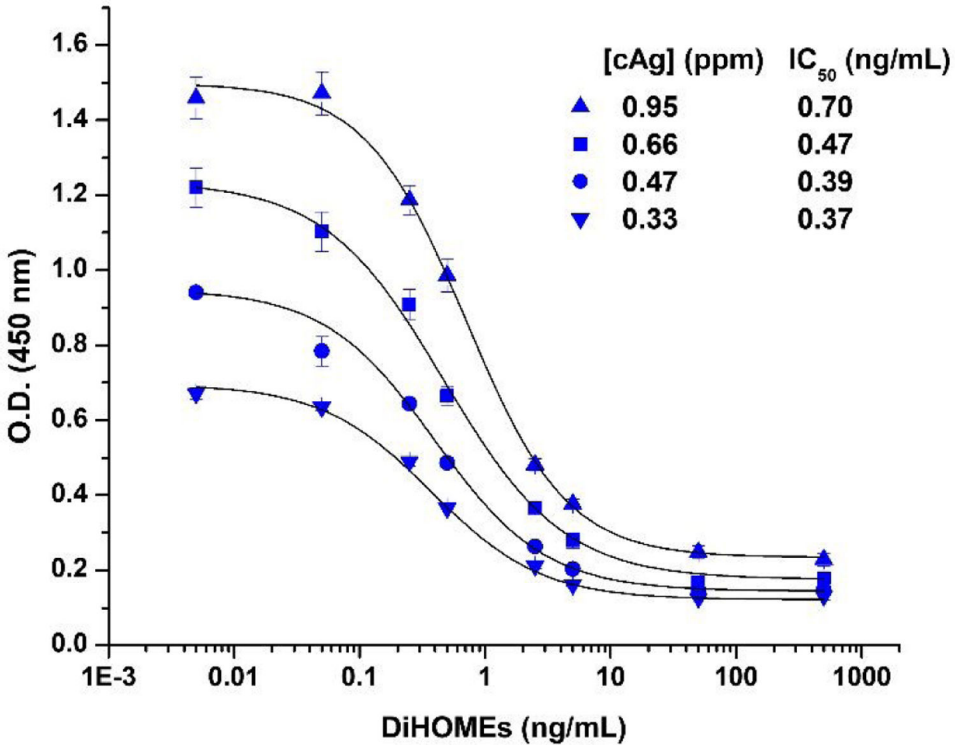

Fig. 4.

Calibration curves (and IC_{50} values) for ELISA format C at varying concentrations of coating antigen (cAg) in neat assay buffer.

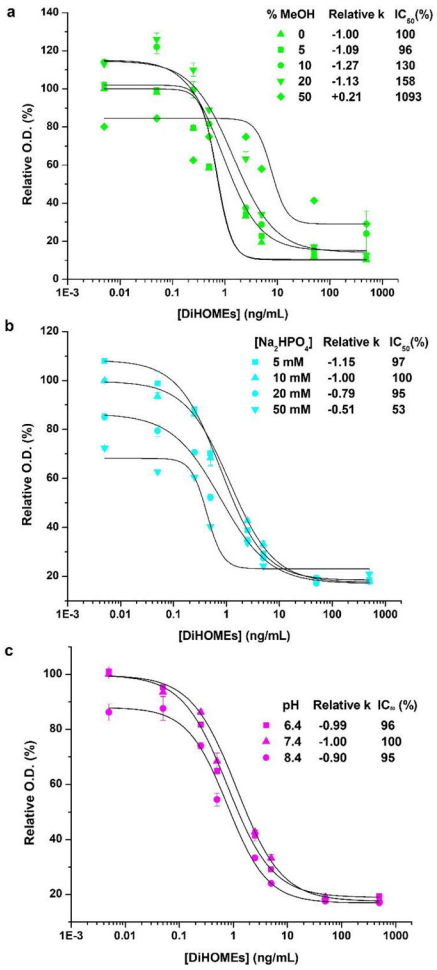

Fig. 5.

Effects of (a) methanol (MeOH), (b) buffer ionic strength, and (c) pH on ELISA performance.

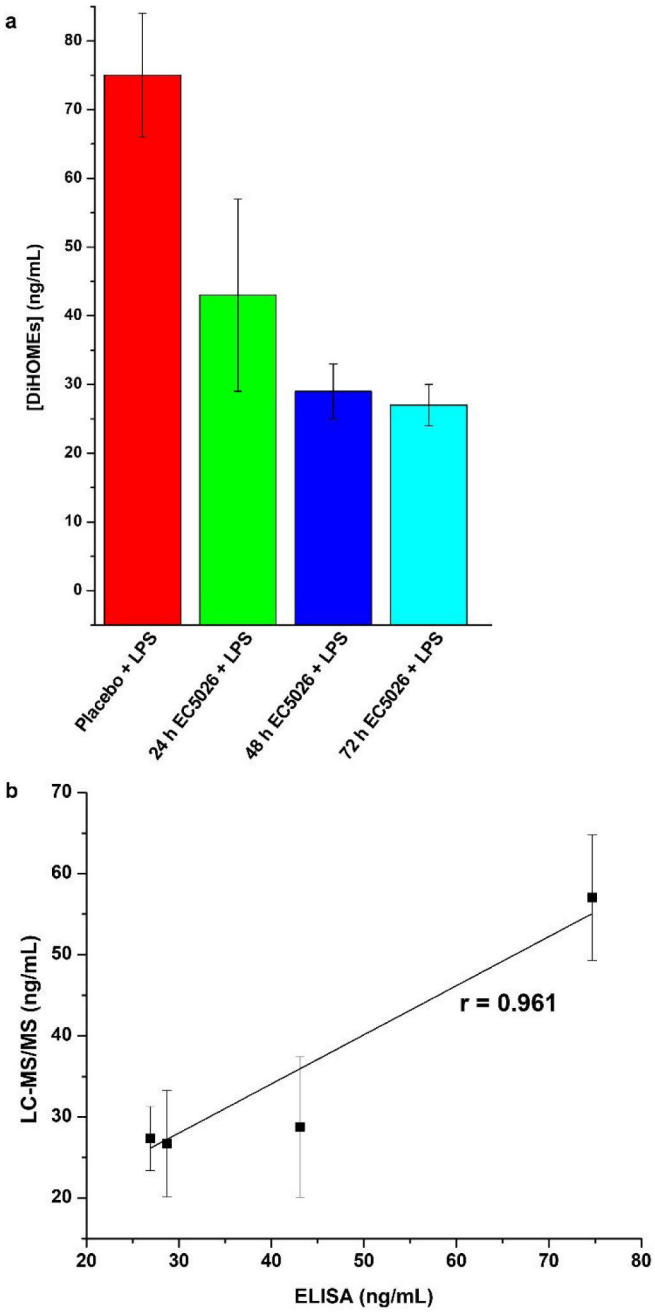

Fig. 6.

Detection of DiHOMEs in clinical samples by the developed ELISA method. (a) DiHOME concentrations (± SD), determined by ELISA, in plasma obtained from four treatment groups (n = 8–16 per group) of a clinical study. (b) Correlation between DiHOME concentrations (± SD) detected by LC-MS/MS and ELISA.

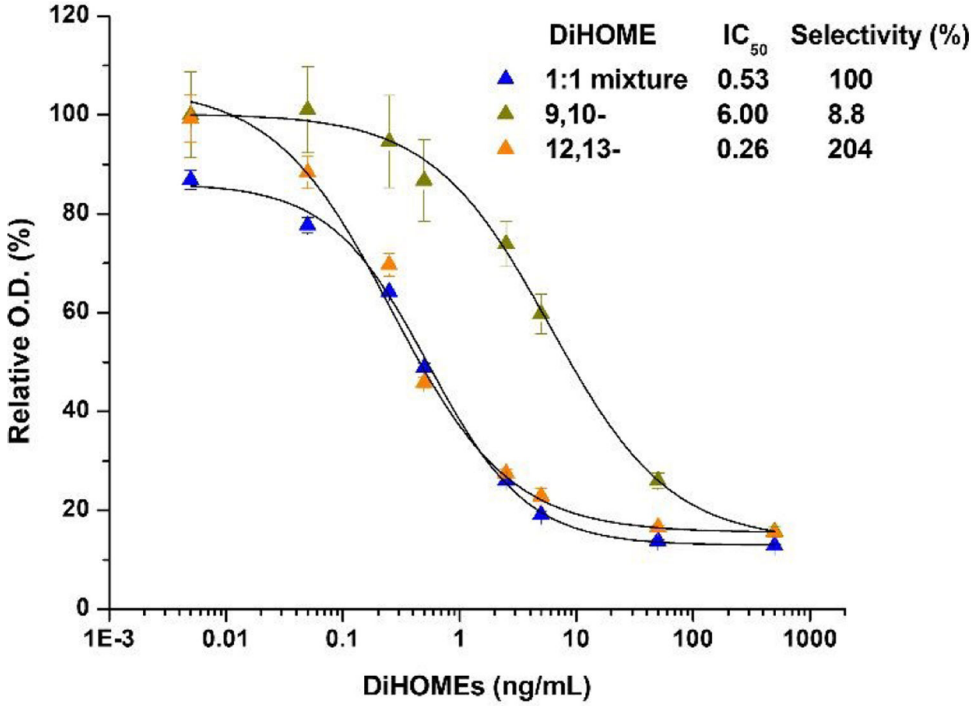

Fig. 7.

Calibration curves for 9,10-DiHOME and 12,13-DiHOME, relative to the DiHOME standard (1:1 regioisomeric mixture), in neat assay buffer.

Table 1

Parameters of logistic and linear fitting of calibration curves for ELISA formats A-C

ELISA Format	Logistic fitting				Linear fitting	
	R^2	LOD (ng/mL)	IC_{50} (ng/mL)	Linear range (IC_{20} – IC_{80}, ng/mL)	Slope (k)	r
A	0.9993	0.11	0.77	0.21 – 2.80	−0.071	−0.9792
B	0.9998	0.13	0.57	0.15 – 2.20	−0.141	−0.9889
C	0.9983	0.11	0.68	0.20 – 2.57	−0.321	−0.9973
B/A	N/A	1.20	0.74	N/A	1.99	N/A
C/A	N/A	1.00	0.88	N/A	4.52	N/A

Table 2

Intra- and inter-assay precision, background, and S/N of ELISA formats A-C

ELISA Format	Precision (CV, %)		Background (%)	S/N
	Intra-assay (*n* = 3)	Inter-assay (*n* = 3)	$O.D._{min}/O.D._{max}$	A1/A2
A	3.40 – 10.9	7.50 – 21.6	18.0	5.62
B	2.71 – 8.44	9.57 – 22.2	13.5	7.32
C	1.44 – 5.02	2.71 – 13.6	16.2	6.05
B/A	N/A	N/A	0.75	1.30
C/A	N/A	N/A	0.9	1.08

Table 3

Cross-reactivity with parent metabolites and mono- and dihydroxy fatty acids

Analyte	Representative structure	Cross-reactivity (%)
LA		< 0.01
EpOMEs[a]		< 0.1
9,10-DiHSA		0.54
THF-diols of LA[a]	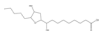	1.19
DiHDPs[a]		6.10
OLE		11.9
DiHODEs[a]		14.3
DiHETs[a]		30.0
DiHDTs[a]		38.7

[a]Regioisomeric mixtures

Table 4

Analytical recovery of DiHOMEs spiked at five concentrations into human plasma

$[DiHOMEs]_{spiked}$ (ng/mL)	$[DiHOMEs]_{measured}$ (ng/mL)	Recovery rate (%)
6.25	6.44	103
12.5	13.5	108
25.0	24.3	97
50.0	55.3	111
100	97.7	98

Table 5

ELISA tolerance to varying concentrations of human plasma

Plasma (%)	0	2.5	5	10	20	25	50
Relative k	−1.00	−1.15	−0.88	−1.13	−0.93	−0.74	−0.42
Matrix Effect (%)[b]	0	+15	−12	+13	−7	−26	−58

[b] + = signal enhancement; − = signal suppression